A Low-Leakage, Low-Loss Magnetic Transformer Structure for High-Frequency Applications

Allen Nguyen, Ajinkya Phanse, Michael Solomentsev, Alex J. Hanson
University of Texas at Austin
2501 Speedway
Austin, USA
Phone: +1 (512) 232-8110
Email: {allentn372}, {ajinkya.phanse}, {mys432}, {ajhanson} @utexas.edu
URL: https://www.utexas.edu/

Acknowledgments

This material is based upon work supported by Enphase Energy.

Keywords

≪Transformer≫, ≪Magnetic device≫, ≪Conduction losses≫, ≪Core loss≫

Abstract

Energy-storage transformers, such as transformers for flyback or LLC converters, have different design constraints than typical transformers. Since primary and secondary currents are not in phase, interleaving does not necessarily reduce high-frequency losses. Such transformers often must be designed with low leakage as well. In this work, we propose design guidelines for a transformer structure that uses field shaping to achieve current conduction along most of the skin of the conductors (double-sided conduction), equal current sharing between paralleled turns, even for out-of-phase currents, and near zero MMF drop across the leakage reluctance paths. The transformer therefore has low leakage inductance and low conduction loss without the use of litz wire and can be used effectively at frequencies beyond a few megahertz. Step-by-step design guidelines are proposed and a prototype transformer is built which achieves a leakage to magnetizing ratio of 1.12%, a power loss $14-17\%$ of a traditional lumped-gap transformer, and current sharing variation less than 1.5% between paralleled turns.

Introduction

Energy-storage transformers must be designed for low conduction loss; but high-frequency effects pose several challenges. Skin depth limitations already lower the effective cross sectional area in which current flows. Then when unbalanced H-fields are present (typically seen with lumped gaps), additional eddy currents within conductors and poor current sharing between parallel conductors can result in orders-of-magnitude higher losses. These adverse high-frequency conduction patterns cannot be mitigated by the use of litz wire above a few MHz where the skin depth becomes thinner than 48 AWG wire [1]. Thus, effective strategies are needed to achieve low conduction loss at MHz frequencies without relying on litz wire.

Energy stored in the leakage inductance of a transformer can also significantly deteriorate the efficiency of a power converter if it is not recovered in each switching cycle. The flyback converter, for example, first stores energy in the magnetizing inductance of the transformer (and inadvertently in the primary leakage) before transferring the magnetizing energy to the output. The energy stored in the leakage is lost if no additional circuitry for recovering the energy is included [2]. For typical leakage-to-magnetizing

inductance ratios (2-5%), this efficiency loss is often unacceptable. Even when the leakage problem is directly addressed through added circuitry, the design of auxiliary leakage-recovery circuits become more constrained for larger leakage inductances. Minimizing leakage inductance is therefore a continuing challenge for many power converter designs.

Leakage is typically reduced by tightly packing ([3, 4]) and/or interleaving the windings. These strategies pose challenges at high frequencies, as tight packing will increase parasitic capacitance [5] and interleaving may not produce good current distributions in energy-storage transformers (such as for flyback or LLC converters) where the primary and secondary current are not in phase.

In this work we propose a low-leakage energy-storage transformer structure for high-frequency applications. The proposed structure uses distributed gaps to shape the H-fields around the conducting wires, resulting in near-zero MMF drops across the core window. This feature forces the flux across the window (leakage) to be near zero, independent of the inter-turn spacing. In addition, the distributed gap balances the H-fields adjacent to two sides of the conductors, even for out-of-phase currents, resulting in a more even distribution of current densities (double-sided conduction) [6]. We use Finite Element Analysis (FEA) simulations to evaluate the transformer and to identify design guidelines. We then test a hardware prototype that achieves a low leakage to magnetizing inductance ratio alongside low power losses and successful current sharing among parallel-connected turns.

Geometry Overview

Fig. 1 shows a cross-section of the proposed transformer structure, which resembles a pot core with a center post, an outer shell, and top and bottom core pieces. Instead of a single air gap, the proposed structure has multiple smaller gaps in both the center post and outer shell that form a quasi-distributed gap [7]. The number of gaps is the same as the number of turns in the transformer, which enables the field-shaping approach proposed in the following sections. The primary and secondary windings of the transformer are interleaved, and each turn of the primary winding is paired with a secondary turn and each such pair is aligned with one core section (for ideal circular turns – we explore the implications of helical turns in the following sections).

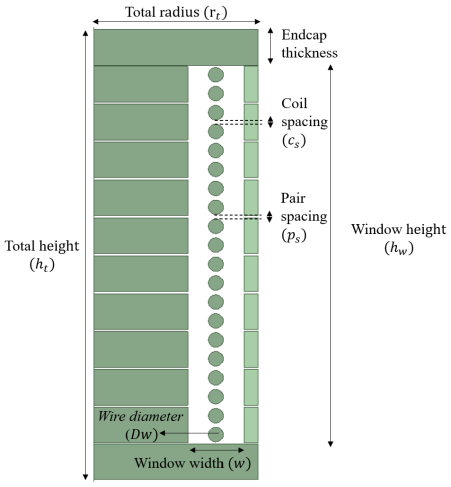

Fig. 1: Radial cross-section of the proposed transformer

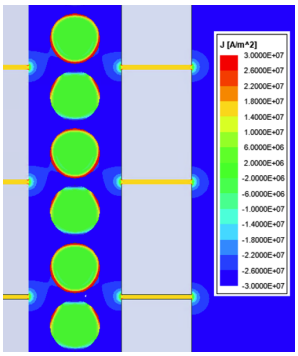

Fig. 2: FEA simulation of balanced H-fields and double-sided conduction

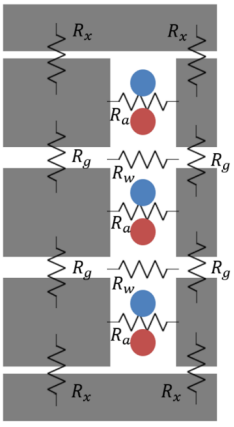

Fig. 3: Transformer showing the various reluctances in the magnetic flux paths

Balanced H-fields for Low Conduction Loss

The introduction of smaller, distributed gaps allows us to strategically manipulate the H-fields around the conductors. The first use of this is to balance the H-fields around each individual conductors. High-frequency current crowds near the conductor edge adjacent to the highest H-field region, increasing copper loss. By balancing the MMF drops across the gaps of the center post and the outer shell we can

achieve balanced H-fields on two sides of the conductor, causing current to evenly distribute on those two sides (known as double-sided conduction [6]). This more even distribution of the current reduces copper losses. An example of balanced H-fields achieving double sided conduction is shown in Fig. 2. This balancing is achieved by making the total reluctance on the center-post equal to the total reluctance in the outer-shell. Fig. 4 shows the lumped reluctance model of the structure. Here, Rc_{post} is the total reluctance of the core pieces in the center post and Rg_{post} is the total reluctance of the air gaps in the center post. Similarly, Rc_{shell} and Rg_{shell} are the reluctances of the core and the air gaps of the outer shell and R_f is the reluctance faced by fields that fringe outside of the structure. Balancing is achieved by enforcing

$$R_{c,post} + R_{g,post} = (R_{c,shell} + R_{g,shell}) || R_f \tag{1}$$

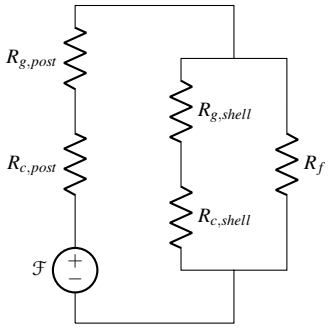

Fig. 4: Magnetic circuit model used to balance the H-fields in the proposed structure

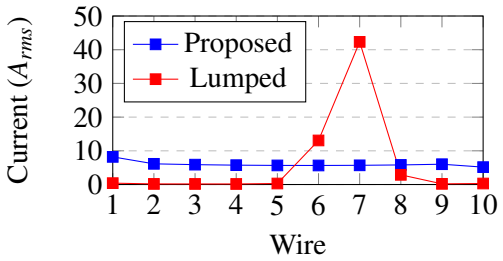

Fig. 5: Current distribution as seen in FEA simulation of the proposed transformer vs. a lumped-gap structure

Double-sided conduction has been achieved in transformers [8], but only for in-phase currents. In this case, double sided conduction is achieved when the currents in the two windings are out of phase (for example, in a flyback converter where only one winding carries current at a time). For high-current or high-turns-ratio transformers, it may also be desirable to arrange multiple turns in parallel. On its own, this can be beneficial for leakage inductance by permitting current to distribute itself to minimize stored energy [5]. However, in the presence of a lumped gap, the current distribution in the paralleled turns can be very uneven, with the turns closest to the region of high H-field carrying the most current.

In the proposed transformer geometry, the turns can be paralleled while still achieving approximately the same net current in each turn. This is a consequence of each conductor pair being in a magnetically similar environment as achieved through the quasi-distributed gap. Fig. 5 shows an FEA comparison between the current distribution in the paralleled turns of the proposed transformer against an identical transformer with a lumped gap (that spanned the center post and outer shell) of the same net reluctance. The proposed approach achieves much better current sharing than the conventional approach, decreasing conduction loss by a very substantial amount. As an example, when the primary is excited with 5 A and the secondary port is open, the conduction loss in the proposed structure was 1.44 W compared to the lumped gap structure with 44.1 W.

MMF Cancellation for Low Leakage Inductance

The quasi-distributed gap structure grants a great deal of design freedom, which we use here to achieve low leakage. We propose to use the many available gaps to balance the MMF drops around the main magnetic path such that the MMF drop across the window (the path of leakage flux through R_w) is zero. Fig. 3 highlights the non-negligible reluctances in different magnetic paths in the proposed structure for a three-turn transformer, with the magnetic circuit equivalent shown in Fig. 6. Each turn of the primary is paired with a turn of the secondary; this will be known as a conducting pair, the space between the primary and secondary turn in a conducting pair will be denoted as conductor spacing (c_s), and the space between conducting pairs will be denoted as pair spacing (p_s). We use the constraint of double-sided conduction to enforce that the reluctance of the center post and the outer shell be equal. For initial

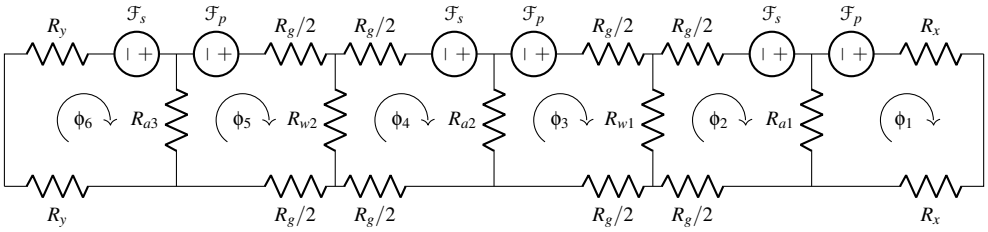

Fig. 6: Magnetic circuit model of the structure shown in Fig. 3

calculations we will assume that there are no large fringing fields outside the structure (i.e assume R_f is negligible) and that only the leakage path associated with the gap between two conducting pairs (R_w) is significant. We will introduce the leakage path associated with the gap between the primary and secondary wire in a conducting pair (R_a) afterwards.

Consider the structure of Fig. 3 excited only by a single winding with the vast majority of flux flowing through the core-and-gap path (not crossing the window). It is plain to see, then, that there will be MMF *gains* traveling up the center post and MMF *drops* traveling down the outer shell. The total MMF gains and drops must be equal; it is therefore conceivable that the sum of the MMF gains and drops around each primary-secondary conductor pair could be engineered to *individually* be zero. This would imply that the MMF drops across the window would also be zero. For this balanced condition, the inclusion of the R_w paths would not change the result because the flux through each R_w would be equal to zero (not just approximately zero). Finally, because the flux across the window (the only flux that does not couple all of the primary and secondary turns) is zero, the leakage inductance must also be zero. In the Appendix, we derive that this such MMF cancellation is possible under the condition that $R_x = R_g/2$.

It is worth dwelling on this conclusion. While most approaches seek to minimize leakage by maximizing *reluctances* associated with leakage (e.g. by tightly packing turns), this approach recognizes the possibility of minimizing the *MMF drop* across such reluctances through judicious balancing of reluctances around the main flux path. In principle, it is possible to reduce the main contributors to leakage inductance to zero. In practice, some flux will be generated locally around each wire and in between the primary/secondary wires, so we expect low but non-zero leakage leakage.

Finite reluctance between the paired primary/secondary turns (R_a in Fig. 3) permits some leakage flux to flow. We examine the effect of R_a numerically by calculating the elements of the inductance matrix through the flux linkage equation, $\underline{\lambda} = \underline{\underline{L}}\,\underline{i}$. When the primary is driven and the secondary is left open, the flux flowing through the V_p MMF sources correspond to the total flux that is linking with the primary winding, for which we adopt the notation (λ_{1po}) [flux linkage in the (1)st (primary) winding with the (p)rimary driven and the other winding (o)pen]. A summary of the open-circuit test equations are shown below.

$$L_{11} = \frac{\lambda_{1po}}{I_1} = \phi_1 + \phi_3 + \phi_5 \qquad L_{22} = \frac{\lambda_{2so}}{I_2} = \phi_2 + \phi_4 + \phi_6 \tag{2}$$

$$L_{12} = \frac{\lambda_{2po}}{I_1} = \phi_2 + \phi_4 + \phi_6 \qquad L_{21} = \frac{\lambda_{1so}}{I_2} = \phi_1 + \phi_3 + \phi_5 \tag{3}$$

$$L_{l,p} = L_{11} - L_{12} \qquad L_{l,s} = L_{22} - L_{21} \tag{4}$$

The previous conclusion that leakage will be zero when $R_x = R_g/2$ is not true anymore and the optimization of gap lengths and expected leakage must be explored. A MATLAB script was written to perform circuit analysis of the magnetic circuit of Fig. 3, with leakages calculated according to the equations above. Fig. 7 shows the variation in the leakage inductance when the gap reluctances that border the end caps (R_x and R_y) are changed while holding constant the reluctances of flux paths through the window (R_a's and R_w's) and the total reluctance of the gaps $(2R_x + 2R_y + 4R_g)$. Thus the variable $R_x/(R_x + R_y)$ becomes a proxy for how symmetric the gaps at the end caps are and $(R_x + R_y)/(R_g/2)$ becomes a proxy for how distributed the air gaps are. Fig. 7 then shows that a symmetric structure, i.e. $R_x = R_y$, is de-

sirable to minimize leakage, though an unbalanced structure does not deviate far from optimal. Fig. 7 also shows that the sum of the primary and secondary port leakages (L_{lkg}) decreases as $(R_x+R_y)/(R_g/2)$ increases. This means that if we are designing a transformer with leakage inductance as a prime design parameter, then a symmetric structure with lumped gaps (and no other gaps) at the endcaps will achieve a lower leakage inductance than the proposed structure. However, the graph is quite flat and rarely are transformers designed considering only the leakage inductance. Instead, the proposed design with $R_x = R_y = R_g/2$ has some important advantages (low leakage achieved alongside better current distributions in the conductors and between paralleled conductors) compared to a structure with lumped gaps near the endcaps. Fig. 8 shows the dependence of L_{lkg} on the window reluctance. Because the

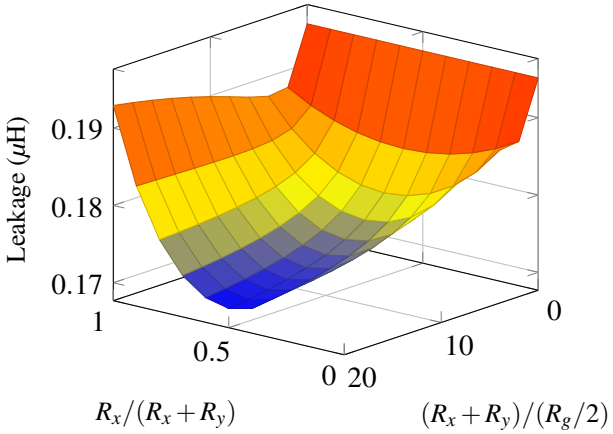

Fig. 7: Leakage inductance as a function of $R_x/(R_x+R_y)$ and $(R_x+R_y)/(R_g/2)$

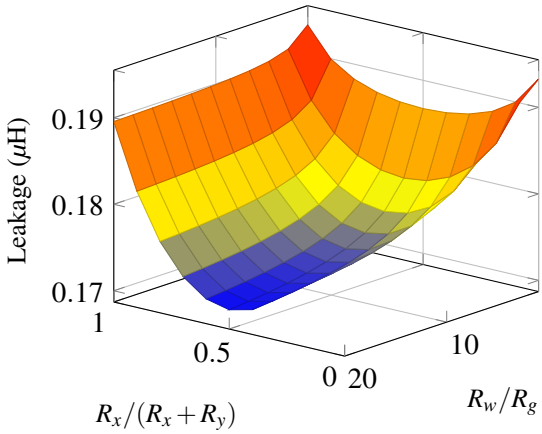

Fig. 8: Leakage inductance as a function of $R_x/(R_x+R_y)$ and R_w/R_g

MMF drop across R_w is close to zero, it can be seen that the leakage path reluctance has little influence on leakage inductance as long as R_w is much greater than R_g. This is expected to be the case in most designs.

Lastly, we introduce simulations to discuss the effect helical turns rather than circular turns such that conductor pairs will not always be centered on their corresponding core piece, as analyzed. To investigate this issue, we run 2-D simulations with windings misaligned from the center of the core (displaced vertically). The leakage inductance is shown to not be sensitive to this misalignment (Fig. 9). Overall, careful placement of the air gaps reduce the leakage inductance of the structure and reduces parameter sensitivities (such as window reluctances and wire placement) on this leakage.

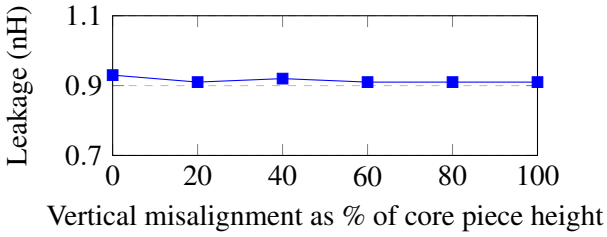

Fig. 9: Total leakage inductance as seen in FEA simulations vs. misalignment of the winding.

Design Guidelines for an Optimized Design

Core Material: Core material selection is application dependent. High-frequency applications are likely to be core loss limited rather than saturation limited and core material is selected based on its performance factor in the desired frequency range as compared in [9].

Number of Turns: The turns ratio and magnetizing inductance are assumed to be set by the application. The total number of turns (and corresponding total core reluctance) is usually chosen by trading off

copper loss and considerations relating to the core (saturation and core loss). When the application is saturation limited, the minimum number of turns consistent with avoiding saturation is used. When the application is core loss limited, an optimal balance between core loss and copper loss is found. High-frequency (MHz) applications are more likely to be core loss limited than saturation limited

The proposed structure uses the same number of conductors for the primary and the secondary. Therefore, for non-unity-turns-ratio transformers, it may be necessary to connect some turns in parallel on the low-turns side. The optimal way to do this may require additional FEA investigation, and may be difficult to optimize for turns ratios in which one side is not a multiple of the other. For example, a 6:3 transformer will have 6 secondary conductors with pairs connected in parallel to form 3 turns (there is still some flexibility to determine which pairs are connected together). By contrast, a 7:3 transformer may have a variety of sensible ways to form 3 turns from 7 conductors on the secondary. For high-current transformers, it is possible to use parallel turns on both the primary and secondary. A 1:1 transformer could have N conductors on both the primary and secondary, all connected in parallel on each side. Nevertheless, for many designs it may be more advantageous to simply use as few parallel-connected wires as possible.

Vertical and Horizontal Fill: For a given window height, large wire diameter restricts the available spacing between adjacent conductors but provides larger conduction area (even in skin-depth-limited designs) leading to lower copper losses. Small space between conductors in a conducting pair causes the little flux that does flow across the window in the conductor spacing region (c_s) to be concentrated with high H-fields, causing current to concentrate in that narrow area. Thus it is important to choose an appropriate wire diameter for a given window height. Fig. 10 and Fig. 11 show the results of simulations

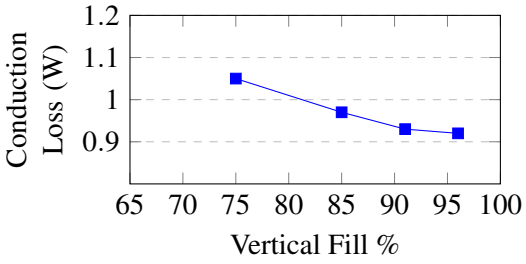

Fig. 10: Conduction losses plotted against vertical fill when c_s is constant p_s is decreased

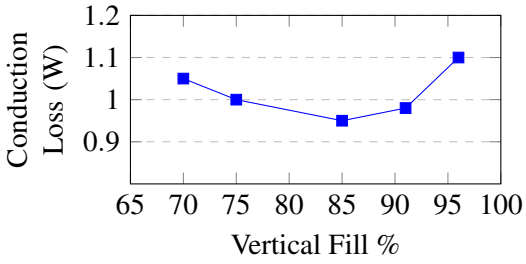

Fig. 11: Conduction losses plotted against vertical fill when p_s is constant c_s is decreased

performed for a 10:10 transformer with an approximately 1:1 aspect ratio (diameter to height). In Fig. 10 the spacing between the conducting wires in a conducting pair (c_s) constant while varying the wire size which is accommodated by varying the spacing between two conducting pairs (p_s). In Fig. 11 we do the opposite, and held p_s constant while varying c_s. While performing these simulations, the width of the window was kept three times the diameter of the biggest wire that would fit (wire corresponding to a vertical fill of 100%) so that the fielding effects due to the changing wire diameter (i.e. R_f, the fields that fridge outside the structure) are negligible. It can be seen that the conduction losses do not increase at higher vertical fill when p_s is decreased (simulated through increased wire diameter). This result is because of the near zero H-field in that region due to the near zero MMF drop across R_w in the window which does not result in any change in current crowding. However, decreasing c_s leads to increased losses. Thus, for a unity turns ratio, it is recommended to have very low pair spacing (p_s) while selecting wire diameter to achieve a vertical fill of $75-90\%$. It may be possible for this spacing to be automatically applied using the insulation of the wires.

Once the wire diameter has been chosen to keep the conduction losses and leakage inductance low, the window width should be chosen such that the total losses in the transformer are minimized. A small window gives more core area and reduces core loss but may expose the wires to fringing fields from the small gaps and increases the leakage flux that flows in the conductor spacing region. Fig. 12 shows the core and copper losses for different horizontal fills (while holding vertical fill at 85% and simulating with a square aspect ratio).

It can be seen that the optima are shallow and maintaining a horizontal fill between $30-60\%$ keeps the total losses low. Larger values of horizontal fill (narrower windows) lead to a larger leakage inductance, incentivizing lower horizontal fill factors for leakage constrained designs. However, this is the conclusion with a square aspect ratio, as shown in the next section, different aspect ratios will require different horizontal fills to reach power loss minimums. Thus we recommend to select the aspect ratio early in the design process.

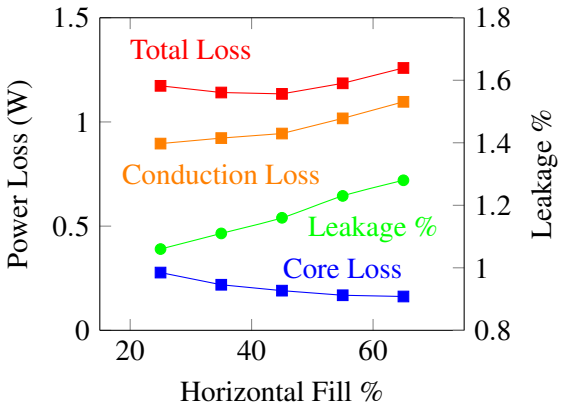

Fig. 12: Power losses observed in FEA simulations for different horizontal fill (all structures had a vertical fill of $\approx 85\%$ and a square aspect ratio)

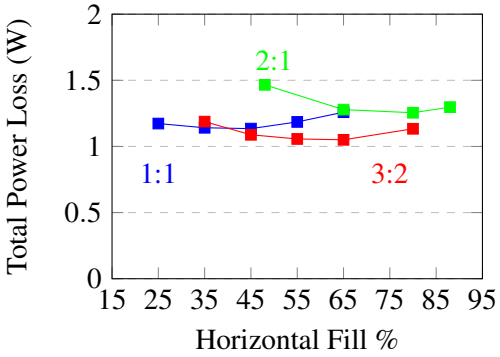

Fig. 13: Total power loss observed in FEA simulations for different Aspect Ratios (all structures had a vertical fill of $\approx 85\%$)

Aspect Ratio: For a given volume, the transformer can have an aspect ratio (height:diameter) that is square (1:1) or it can be tall and skinny or short and wide. This design choice has several implications for other aspects of the design, such as wire length, wire spacing, gap length, etc. For example, a taller structure would allow the use of wires with larger diameters for the same vertical fill resulting in lower copper losses, but would result in smaller core cross-sectional area, increasing core losses. To observe the effect of the aspect ratio, we ran several simulations of transformers with the same volume and different aspect ratio while optimizing the horizontal fill (window width) under the same vertical fill ($\approx 85\%$). As observed by Fig. 13, relatively square aspect ratios are preferred, with the optimal closer to 1.5:1.

Gap Lengths: Since magnetizing inductance and number of turns have been fixed, the number of gaps and the gap size are determined from the center post area and the outer shell area (with an optional correction factor to account for fringing fields).

End Caps: The choice of end cap size is a trade off between cross-sectional area (height) and transformer volume. The trade off is not linear, however, as flux tends to crowd near the edges of the window. It is recommended to start the design process with a reasonable end cap height, then tune the height of the end caps after the choice of the center-post radius, outer-shell thickness and wire diameter have been made. Fig. 14 below shows the comparison between the end cap volume to the end cap core loss contribution.

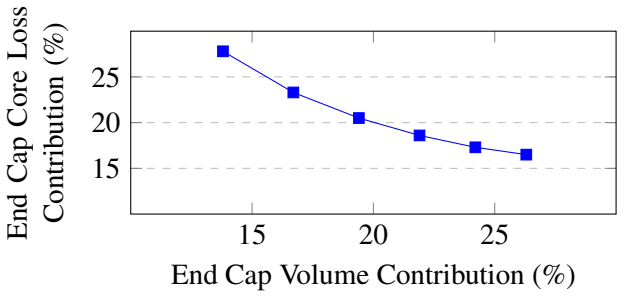

Fig. 14: Increasing end cap thickness and its effects on lowering core loss

This figure shows as the percentage of end cap volume to the total volume ($volume_{endcap}/volume_{total}$) is increased past $\approx 25\%$, the reduction in core loss is not substantial. For near-square aspect ratio transformers, end cap volumes between $20-25\%$ are likely to keep the core loss contribution of the end caps low without adding too much volume.

Prototype Design and Test Results

In order to validate the design procedure outlined above, a 1:1 and a 1:10 transformer with parallel turns were built at a target magnetizing inductance of 11 μH with a desired operating frequency of 2 MHz. The transformer was designed under a volume constraint of $< 1in^3$ with a target 3:2 aspect ratio, a $\sim$88.5% vertical fill, and a $\sim$55% horizontal fill.

Design Parameters: First, due to its high performance factor at 2-3 MHz [9, 10], Fair-Rite 80 was chosen for all core pieces (center post discs, end caps, and outer shell pieces) of the transformer.

As for geometric considerations, the volume and aspect ratio selection gave us an initial transformer diameter of 23 mm and a height of 34.5 mm. We then initially set the end cap lengths to be 4.25 mm each. Thus the window height is 26 mm. Then, because of this window height and the selected vertical fill, 17 AWG magnet wire was selected as the conducting material. Then, to achieve the selected horizontal fill given the 17 AWG wire, the widow width was selected to be 2.1 mm.

Now, in order to ensure that the H-fields on each side of the conductor are balanced and that we minimize leakage inductance, the end cap gap lengths were set to be equal to each other ($R_x = R_y$) and set to be half the length of the center post and shell gap lengths ($R_x = R_g/2$). This, alongside the target magnetizing inductance of ≈ 11 μH, the total of ten conducting pairs, and the area selection, we required that the end cap gap lengths (R_x, R_y) are 50 μm, and the center post and shell gaps (R_g) are 100 μm. This selection alongside the window height, required that each core section of the center post and the outer shell to be 2.5 mm.

Lastly, after simulating this transformer, the end cap length's were decreased to 3.5 mm to reduce volume, without significantly impacting simulated core loss values. Table I below summarizes all of the design parameters.

Table I: Geometry and specifications of the simulated transformer

Parameter	Value	Unit
Magnetizing Inductance	11	μH
Total Diameter	23	mm
Total Height	33	mm
Center Post Diameter	15.6	mm
Window Height	26	mm
Window Width	2.1	mm
Core Section Height	2.5	mm
End Cap Height	3.5	mm
End Cap Gap Lengths	50	μm
Center Core Gap Lengths	100	μm
Wire Selection	17	AWG

Fig. 15: (left) Shell construction on a half-cylindrical jig. (middle) Disassembled modules of the transformer. (right) Final built transformer.

Prototype Construction: The transformer core consists of several different segments: the center post, the outer shells, the end caps, and the windings. The center post was constructed by stacking center post disks with laser-cut shim stock spacers at the optimized gap height in between them. The outer shell was constructed in the same manner. Due to the C shape of the shells, a half cylindrical jig was used to assist in the construction as shown in Fig. 15.

During construction, the center post and shell height were increased in order to account for the helical nature of the windings, this change adjusted both the aspect ratio ($\sim$3:2 $\rightarrow$ $\sim$5:3) and the vertical fill

value (88.5% $\rightarrow$ 75%) and was accounted for in simulated results. Also for ease of construction, we kept the pair and coil spacing constant to allow the insulation of the wires to provide the spacing between conductors.

Inductance Measurements: The 1:1 transformer's inductances were measured through a E5061B Network Analyzer using open- and short-circuit one-port measurements, with results in Table II. These values then allow us to calculate the ratio of the leakage inductance to the magnetizing inductance, with results in Table III.

Table II: Constituent inductances for the proposed transformer, experimental and simulated

	Measured (μH)	Simulation (μH)
Lm	9.324	11.386
L11	9.389	11.456
L22	9.429	11.446

Table III: Leakage to magnetizing inductance ratios for the proposed transformer

	Measured	Simulation
Ll1/Lmag	0.70%	0.62%
Ll2/Lmag	1.12%	0.53%

Port inductance measurements do vary ($\sim$ 18%) from simulation, which could be due to structural changes and defects associated with prototyping (such as non-ideal, gap spacing due to the curled edges of the laser cut plastic spacers). However, the prototype transformer does achieves a low leakage to magnetizing ratio of 0.70% on the primary port and a ratio of 1.12% on the secondary. Also, through the network analyzer, we measured a resonant frequency of the structure around 20 MHz, indicating that the structure also achieves a low parasitic capacitance.

Power Loss Measurements: The power losses of the transformer were measured on the primary and the secondary windings through a series resonant based approach [11, 12]. This technique allows for accurate loss measurements at high-frequency by measuring only sinusoidal voltage amplitudes. These results are found in Table IV and Table VI, both showing good agreement with simulation across different current drives (validating this method as a form of loss measurement).

Table IV: Primary side power losses for the prototype 1:1 transformer, values measured at 1.918 MHz

Current (A)	Measured (W)	Simulation (W)	Error
1.59	0.254	0.273	6.95%
2.04	0.429	0.475	9.63%
2.38	0.600	0.662	9.29%

Table V: Primary side power losses for a lumped-gap equivalent, values measured at 1.965 MHz

Current (A)	Measured (W)
1.61	1.602
2.03	2.502
2.44	3.574

Table VI: Secondary side power losses for the prototype 1:1 transformer, values measured at 1.916 MHz

Current (A)	Measured (W)	Simulation (W)	Error
1.62	0.253	0.265	4.71%
1.99	0.385	0.412	6.57%
2.37	0.558	0.618	9.85%

Table VII: Secondary side power losses for a lumped-gap equivalent, values measured at 1.947 MHz

Current (A)	Measured (W)
1.59	1.689
1.98	2.614
2.37	3.810

We also used the same power loss measurements on an identical transformer with a lumped gap in the center post and the outer shell as opposed to the distributed gap of the proposed structure. These results are found in Table V and Table VII. Overall, the lumped gap transformer had $6-7$ times the amount of measured loss as compared to our prototype design.

Current Sharing: Lastly, to verify that each wire was in a magnetically similar environment and could share current as predicted, we tested a 10:1 structure where the paralleled one-turn port (secondary) turns

were interleaved with the ten-turn port (primary) turns. This winding procedure resulted in ten separate paralleled current paths spaced evenly across the length of the transformer. Driving the primary of this transformer allowed us to measure the current from each of the secondary paths resulting in Fig. 16 below.

Experimentally, the percentage of the net current in each parallel turn ranged from 8.5% to 10.9%, indicating successful current sharing.

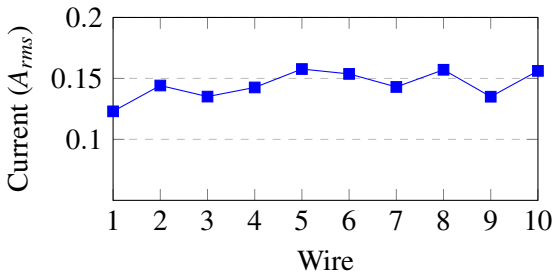

Fig. 16: Current measured from each paralleled wire in the prototype transformer

Conclusion

In this work we proposed a low loss, low leakage transformer that is suitable for application in high frequency power converters. The transformer achieves low conduction losses by balancing the H-fields on the two sides of the windings so that the current flows along nearly the entire skin of the conductor. Distributed gaps shape the H-fields such that each turn of the transformer windings are in a magnetically similar environment. This allows paralleling of the turns of the transformer winding such that each turn carries almost equal current. These properties make the transformer especially suitable for applications with large currents and requiring high turns ratios. The proposed structure also achieves almost zero MMF drop across the window. Because of this, the transformer achieves a very small leakage inductance. This low leakage inductance enables the use of this transformer structure in power converters like coupled-inductor boost or flyback converters which would otherwise require additional circuitry to recover the energy stored in the leakage inductance. The design guidelines provided in this work were confirmed experimentally with a prototype transformer of which achieved both low losses and a low leakage to magnetizing inductance ratio.

Appendices

Derivation to reduce MMF drop across R_w to zero: For the magnetic circuit model, $\mathcal{F}_p$ is the MMF introduced by each primary turn, $\mathcal{F}_s$ is the MMF introduced by each primary turn, and ϕ_i are fluxes in the magnetic circuit meshes (in Fig. 6, six meshes are shown for illustration). We first analyze the magnetic circuit without the parasitic leakage path in between the paired primary/secondary turn, R_a. For an n-stage network, the MMF drop across the i^{th} window reluctance R_w can be given by the sum of the MMF contributions by the sources on the right of the i^{th} R_w ($\mathcal{F}\{R_{w_i}\}_{right}$) and those on its left ($\mathcal{F}\{R_{w_i}\}_{left}$).

$$\mathcal{F}\{R_{w_i}\}_{right} = \frac{((i-1)(2R_g)+R_z)}{2R_z+(n-2)(2R_g)}(n-i)\mathcal{F}_p \tag{5}$$

$$\mathcal{F}\{R_{w_i}\}_{left} = \frac{(((n-2)-(i-1))(2R_g)+R_z)}{2R_z+(n-2)(2R_g)}(i)(-\mathcal{F}_p) \tag{6}$$

Here, R_z is equal to $2R_x+R_g$. Then by setting $|\mathcal{F}\{R_{w_i}\}_{right}| = |(\mathcal{F}\{R_{w_i}\}_{left}|$, we find that the MMF drop across R_{w_i} becomes zero when $R_x = R_g/2$. Thus, if the length of air gap at the endcaps is half of the length of air gap in the center post, we get zero flux through the window reluctances.

References

[1] C. R. Sullivan, “Prospects for advances in power magnetics,” Proc. 9th Int. Conf. Integr. Power Electron. Syst., 2016

[2] Q. Zhao and F. Lee, “High-efficiency, high step-up dc-dc converters,” IEEE Transactions on Power Electronics, vol. 18, no. 1, pp. 65–73, 2003.

[3] B. Tamyurek and D. A. Torrey, “A three-phase unity power factor single-stage ac–dc converter based on an interleaved flyback topology,” IEEE Transactions on Power Electronics, vol. 26, no. 1, pp. 308–318, 2011.

[4] B. Tamyurek and B. Kirimer, “An interleaved high-power flyback inverter for photovoltaic applications,” IEEE Transactions on Power Electronics, vol. 30, no. 6, pp. 3228–3241, 2015.

[5] Z. Ouyang, O. C. Thomsen, and M. A. E. Andersen, “The analysis and comparison of leakage inductance in different winding arrangements for planar transformer,” in 2009 International Conference on Power Electronics and Drive Systems (PEDS), 2009, pp. 1143–1148.

[6] R. S. Yang, A. J. Hanson, D. J. Perreault, and C. R. Sullivan, “A low-loss inductor structure and design guidelines for high-frequency applications,” in 2018 IEEE Applied Power Electronics Conference and Exposition (APEC), 2018, pp. 579–586.

[7] J. Hu and C. Sullivan, “The quasi-distributed gap technique for planar inductors: design guidelines,” in IAS ’97. Conference Record of the 1997 IEEE Industry Applications Conference Thirty-Second IAS Annual Meeting, vol. 2, 1997, pp. 1147–1152 vol.2.

[8] O. Okeke, M. Solomentsev and A. J. Hanson, ”Double-Sided Conduction: A Loss-Reduction Technique for High Frequency Transformers,” 2022 IEEE Applied Power Electronics Conference and Exposition (APEC), 2022.

[9] A. J. Hanson, J. A. Belk, S. Lim, C. R. Sullivan, and D. J. Perreault, “Measurements and performance factor comparisons of magnetic materials at high frequency,” IEEE Transactions on Power Electronics, vol. 31, no. 11, pp. 7909–7925, 2016.

[10] High Frequency Power Materials, Fair-Rite Products Corp., 2 2018.

[11] Y. Han, G. Cheung, A. Li, C. R. Sullivan, and D. J. Perreault, “Evaluation of magnetic materials for very high frequency power applications,” IEEE Transactions on Power Electronics, vol. 27, no. 1, pp. 425–435, 2012.

[12] M. Solomentsev, O. Okeke and A. J. Hanson, ”A Resonant Approach to Transformer Loss Characterization,” 2022 IEEE Applied Power Electronics Conference and Exposition (APEC), 2022